

# Soft-gluon resolution scale in QCD evolution equations

F. Hautmann<sup>a,b,c</sup>, H. Jung<sup>d</sup>, A. Lelek<sup>d</sup>, V. Radescu<sup>e</sup>, R. Žlebčík<sup>d</sup>

<sup>a</sup>Rutherford Appleton Laboratory, Chilton OX11 0QX

<sup>b</sup>Theoretical Physics Department, University of Oxford, Oxford OX1 3NP

<sup>c</sup>Elementaire Deeltjes Fysica, Universiteit Antwerpen, B 2020 Antwerpen

<sup>d</sup>Deutsches Elektronen Synchrotron, D 22603 Hamburg

<sup>e</sup>CERN, CH-1211 Geneva 23

---

## Abstract

QCD evolution equations can be recast in terms of parton branching processes. We present a new numerical solution of the equations. We show that this parton-branching solution can be applied to analyze infrared contributions to evolution, order-by-order in the strong coupling  $\alpha_s$ , as a function of the soft-gluon resolution scale parameter. We examine the cases of transverse-momentum ordering and angular ordering. We illustrate that this approach can be used to treat distributions which depend both on longitudinal and on transverse momenta.

---

The evolution of QCD parton cascades is an essential element of theoretical predictions for production processes with high momentum transfer at high-energy colliders. It has been realized since long that realistic predictions for collider processes require taking into account contributions to QCD evolution not only from collinear parton radiation, associated with the renormalization group behavior at high momenta, but also from soft gluon radiation, including its color coherence properties [1–5]. Infrared radiation contributions are controlled by a finite resolution scale  $\delta$  of order  $\delta \sim O(\Lambda_{\text{QCD}}/\mu)$ , where  $\mu$  is the hard scattering scale and  $\Lambda_{\text{QCD}} \approx 1 \text{ fm}^{-1}$  is the natural scale of strong interactions.

In this paper we study the effects of soft-gluon emission and the soft-gluon resolution scale in cases in which not only longitudinal-momentum degrees of freedom but also transverse-momentum degrees of freedom are necessary for reliable theoretical predictions. We address the issue of taking into account simultaneously soft gluon radiation, with light-cone momentum fraction  $z \rightarrow 1$ , and transverse momentum  $\mathbf{q}_\perp$  recoils in the parton branchings along the QCD cascade. This is relevant for instance in multiple-scale problems, such as the high invariant-mass region of heavy particle spectra and the high-energy limit of hadroproduction processes, where transverse-momentum dependent (TMD) factorization theorems apply (see e.g. [6] for a recent review).

While analytic resummation methods exist, based on these theorems, for sufficiently inclusive variables such as, e.g., heavy-boson transverse spectra, the viewpoint in this work is to aim at a formulation by which one could also treat exclusive components of the final states. Parton-shower algorithms do provide such a formulation, and are widely used as an effective alternative (though limited in accuracy) to analytic resummation methods. While great progress has been achieved in the last decade on matching and merging methods [7] to combine parton showers with perturbative calculations through next-to-leading order, several open questions still remain, both conceptual and technical, on the appropriate use of parton distribution functions in parton showers [8] and on the treatment of the shower’s transverse momentum kinematics [9].

In the context of analytic methods, the behavior of parton distributions near the endpoint  $z \rightarrow 1$  motivates the use of infrared subtractive techniques which lead to a generalization of the “plus” distribution [10] including transverse degrees of freedom. In this paper we describe a new calculation, based on the unitarity method [1] to recast evolution equations in terms of Sudakov form factors and real emission kernels, and present a study of the soft-gluon resolution

scale in the cases of inclusive parton distributions and of transverse-momentum dependent parton distributions. We analyze different ordering variables, including transverse momentum ordering and angular ordering. The method set up in this paper can be applied systematically order-by-order in the strong coupling  $\alpha_s$ , at leading order as well as at next-to-leading and higher orders. In this article we present the basic results and numerical leading-order applications. Details of the method and applications including next-to-leading order will be presented elsewhere [11].

We start from the renormalization group evolution of parton distribution functions [12–14]

$$\frac{\partial \widetilde{f}_a(x, \mu^2)}{\partial \ln \mu^2} = \sum_b \int_x^1 dz P_{ab}(\alpha_s(\mu^2), z) \widetilde{f}_b(x/z, \mu^2) . \quad (1)$$

where  $\widetilde{f}_a(x, \mu^2) \equiv x f_a(x, \mu^2)$  are momentum-weighted parton distributions for  $a = 1, \dots, 2N_f + 1$  species of partons (with  $N_f$  the number of quark flavors) as functions of longitudinal momentum fraction  $x$  and evolution mass scale  $\mu$ , and  $P_{ab}(\alpha_s, z)$  are splitting functions, computable as perturbation series expansions in powers of the strong coupling  $\alpha_s$ .

We classify the singular behavior of the splitting functions  $P_{ab}(\alpha_s, z)$  for  $z \rightarrow 1$  according to the decomposition

$$P_{ab}(\alpha_s, z) = D_{ab}(\alpha_s) \delta(1-z) + K_{ab}(\alpha_s) \frac{1}{(1-z)_+} + R_{ab}(\alpha_s, z) , \quad (2)$$

where the plus-distribution  $1/(1-z)_+$  is defined for any test function  $\varphi$  as

$$\int_0^1 \frac{1}{(1-z)_+} \varphi(z) dz = \int_0^1 \frac{1}{1-z} [\varphi(z) - \varphi(1)] dz . \quad (3)$$

Eq. (2) decomposes the splitting functions into the  $\delta(1-z)$  distribution, the  $1/(1-z)_+$  distribution, and the function  $R_{ab}(\alpha_s, z)$  which contains logarithmic terms in  $\ln(1-z)$  and analytic terms for  $z \rightarrow 1$ . The  $\delta(1-z)$  and  $1/(1-z)_+$  contributions to splitting functions are diagonal in flavor,

$$D_{ab}(\alpha_s) = \delta_{ab} d_a(\alpha_s) , \quad K_{ab}(\alpha_s) = \delta_{ab} k_a(\alpha_s) \quad (4)$$

(no summation over repeated indices). The constants  $d_a$  and  $k_a$  and the functions  $R_{ab}$  in Eq. (2) can be expanded in powers of  $\alpha_s$ . The two-loop expansions for the constants  $d_a$  and  $k_a$  may be obtained from [15, 16] and read

$$\begin{aligned} d_q &= \frac{3\alpha_s C_F}{4\pi} + \left(\frac{\alpha_s}{2\pi}\right)^2 \left[ C_F^2 \left( \frac{3}{8} - \frac{\pi^2}{2} + 6\zeta(3) \right) + C_F C_A \left( \frac{17}{24} + \frac{11\pi^2}{18} - 3\zeta(3) \right) - C_F T_R N_f \left( \frac{1}{6} + \frac{2\pi^2}{9} \right) \right] + \mathcal{O}(\alpha_s^3) , \\ d_g &= \frac{\alpha_s}{2\pi} \left( \frac{11}{6} C_A - \frac{2}{3} T_R N_f \right) + \left(\frac{\alpha_s}{2\pi}\right)^2 \left[ C_A^2 \left( \frac{8}{3} + 3\zeta(3) \right) - \frac{4}{3} C_A T_R N_f - C_F T_R N_f \right] + \mathcal{O}(\alpha_s^3) , \\ k_q &= \frac{\alpha_s C_F}{\pi} + \frac{\alpha_s^2 C_F}{2\pi^2} \Gamma + \mathcal{O}(\alpha_s^3) , \quad k_g = \frac{\alpha_s C_A}{\pi} + \frac{\alpha_s^2 C_A}{2\pi^2} \Gamma + \mathcal{O}(\alpha_s^3) , \quad \Gamma \equiv C_A \left( \frac{67}{18} - \frac{\pi^2}{6} \right) - T_R N_f \frac{10}{9} , \end{aligned} \quad (5)$$

where  $C_A = N_c$ ,  $C_F = (N_c^2 - 1)/(2N_c)$ ,  $T_R = \frac{1}{2}$  are  $SU(N_c)$  color factors ( $N_c = 3$ ), and  $\zeta$  is the Riemann zeta function. Analogously, explicit expressions for the functions  $R_{ab}$  may be obtained from [15, 16] through two loops.

In the physical picture of Eqs. (1),(2) a finite resolution scale in the transverse distance between emitted partons implies, by energy-momentum conservation, that partons radiated with longitudinal momentum fractions closer to  $z = 1$  than a certain cut-off value,  $z > z_M$  with  $1 - z_M \sim \mathcal{O}(\Lambda_{\text{QCD}}/\mu)$ , cannot be resolved. Removing such radiative contributions from the evolution, on the other hand, leads to a violation of unitarity. The key idea of the parton branching method is to restore unitarity by recasting the evolution equations in terms of no-branching probabilities (Sudakov form factors) and real-emission branching probabilities [1, 17].

To this end, in this work we proceed in two steps, as follows. First, we introduce the resolution scale parameter  $z_M$  into the evolution equations (1) by splitting the integration range on the right hand side into the resolvable ( $z < z_M$ ) and non-resolvable ( $z > z_M$ ) regions. We include terms through  $\mathcal{O}(1 - z_M)^0$  but neglect power-suppressed contributions  $\mathcal{O}(1 - z_M)^n$ ,  $n \geq 1$ . (The details of this analysis will be given elsewhere [11].) Further we use the momentum sum rule

$$\sum_c \int_0^1 z P_{ca}(\alpha_s, z) dz = 0 \quad (\text{for any } a) \quad (6)$$

to systematically eliminate  $D$ -terms in Eq. (2) in favor of  $K$ - and  $R$ -terms. Then the evolution equations (1) can be recast in integral form as

$$\begin{aligned} \widetilde{f}_a(x, \mu^2) &= S_a(z_M, \mu^2, \mu_0^2) \widetilde{f}_a(x, \mu_0^2) + \sum_b \int_{\mu_0^2}^{\mu^2} \frac{d\mu'^2}{\mu'^2} \frac{S_a(z_M, \mu^2, \mu_0^2)}{S_a(z_M, \mu'^2, \mu_0^2)} \\ &\times \int_x^{z_M} dz \left( K_{ab}(\alpha_s(\mu'^2)) \frac{1}{1-z} + R_{ab}(\alpha_s(\mu'^2), z) \right) \widetilde{f}_b(x/z, \mu'^2) + \mathcal{O}(1-z_M), \end{aligned} \quad (7)$$

where  $S_a$  is the Sudakov form factor

$$S_a(z_M, \mu^2, \mu_0^2) = \exp \left[ - \sum_b \int_{\mu_0^2}^{\mu^2} \frac{d\mu'^2}{\mu'^2} \int_0^{z_M} dz z \left( K_{ab}(\alpha_s(\mu'^2)) \frac{1}{1-z} + R_{ab}(\alpha_s(\mu'^2), z) \right) \right]. \quad (8)$$

Eqs. (7),(8) take into account the effects of the  $d$ -terms in Eq. (5) and subtraction term in Eq. (3) implicitly, while the  $k$ -terms in Eq. (5) (as well as the  $R$ -terms) are integrated over up to the resolution scale parameter  $z_M$ .

Next, we solve Eq. (7) by numerical Monte Carlo method and use the parton branching kinematics (Fig. 1) to relate the transverse momentum recoils at each branching to the evolution variable. With reference to the notation of Fig. 1 for the splitting  $b \rightarrow a + c$ , the plus lightcone momenta are  $p_a^+ = zp_b^+$ ,  $p_c^+ = (1-z)p_b^+$ . We consider the cases of transverse-momentum ordering and angular ordering [18, 19]. In the first case we have

$$\mu = |\mathbf{q}_c|, \quad (9)$$

where  $\mathbf{q}_c$  is the (euclidean) transverse momentum vector of particle  $c$ . In the second case we have

$$\mu = |\mathbf{q}_c|/(1-z). \quad (10)$$

For numerical solution, we develop a new program based on the Monte Carlo method which was earlier employed

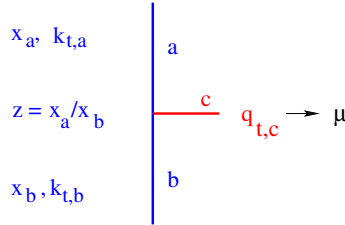


Figure 1: Branching process  $b \rightarrow a + c$ .

by some of us for studies of the CCFM equations [20, 21]. The application to the case of the evolution equations (7)<sup>1</sup> presents different features with respect to the CCFM case. These depend especially on the different flavor structure of the two equations, and the different behavior of the kernels at small longitudinal momentum fractions. While CCFM equations are dominated by the gluon channel, Eq. (7) has fully coupled flavor structure. The small- $x$  behavior of CCFM kernels is controlled by the non-Sudakov form factor. In the case of Eq. (7) it is essential to work with momentum-weighted distributions to improve the convergence of the numerical integration over the region of small  $x$ . The iterative solution of Eq. (7) schematically reads

$$\widetilde{f}_a(x, \mu^2) = \sum_{i=0}^{\infty} \widetilde{f}_a^{(i)}(x, \mu^2), \quad (11)$$

<sup>1</sup>First results from this numerical program have been presented in [22].

where

$$\begin{aligned}
\tilde{f}_a^{(0)}(x, \mu^2) &= S_a(z_M, \mu^2, \mu_0^2) \tilde{f}_a(x, \mu_0^2), \\
\tilde{f}_a^{(1)}(x, \mu^2) &= \sum_b \int_{\mu_0^2}^{\mu^2} \frac{d\mu'^2}{\mu'^2} \frac{S_a(z_M, \mu^2, \mu_0^2)}{S_a(z_M, \mu'^2, \mu_0^2)} \int_x^{z_M} dz S_b(z_M, \mu'^2, \mu_0^2) \\
&\quad \times \left( K_{ab}(\alpha_s(\mu'^2)) \frac{1}{1-z} + R_{ab}(\alpha_s(\mu'^2), z) \right) \tilde{f}_b(x/z, \mu_0^2), \dots
\end{aligned} \tag{12}$$

Using this branching Monte Carlo solution and the parton kinematic relations given above, we are able to compute the distribution  $\mathcal{A}_a$  in the transverse momentum  $\mathbf{k} = -\sum_c \mathbf{q}_c$ , in addition to the inclusive distribution, integrated over  $\mathbf{k}$ ,

$$\int x \mathcal{A}_a(x, \mathbf{k}, \mu^2) \frac{d^2 \mathbf{k}}{\pi} = \tilde{f}_a(x, \mu^2). \tag{13}$$

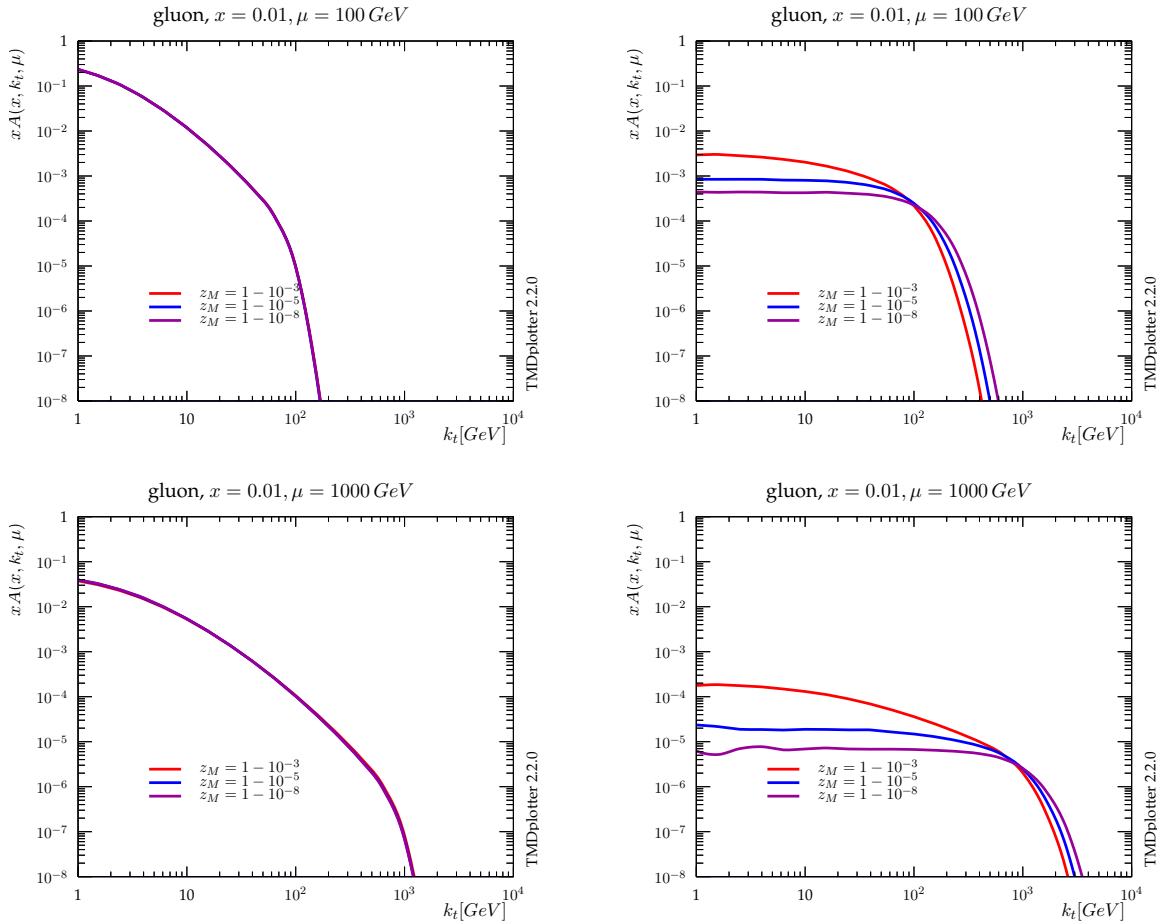


Figure 2: Transverse momentum gluon distribution at  $x = 10^{-2}$  and  $\mu = 100$  GeV (upper row),  $\mu = 1000$  GeV (lower row) for different values of the resolution scale parameter  $1 - z_M = 10^{-3}, 10^{-5}, 10^{-8}$ : (left) angular ordering; (right) transverse momentum ordering.

The key observation is that while in the case of the inclusive distribution the cancellation of real and virtual non-resolvable emissions leads to results which become independent of the resolution parameter  $z_M$  for large enough

$z_M$ , regardless of the choice of the evolution variable, the case of the transverse momentum distribution is infrared-sensitive and depends on the appropriate choice of the evolution variable (e.g., Eqs. (9),(10)). In the framework of [10], this infrared sensitivity is treated by using the subtractive technique [23] in the definition of transverse momentum dependent distributions and leads to a generalization of the plus distribution (3). In the case of the branching solution of the evolution equations analyzed in this paper, we will see next that the angular ordering (10) takes into account the cancellation of non-resolvable emissions and gives stable,  $z_M$ -independent results.

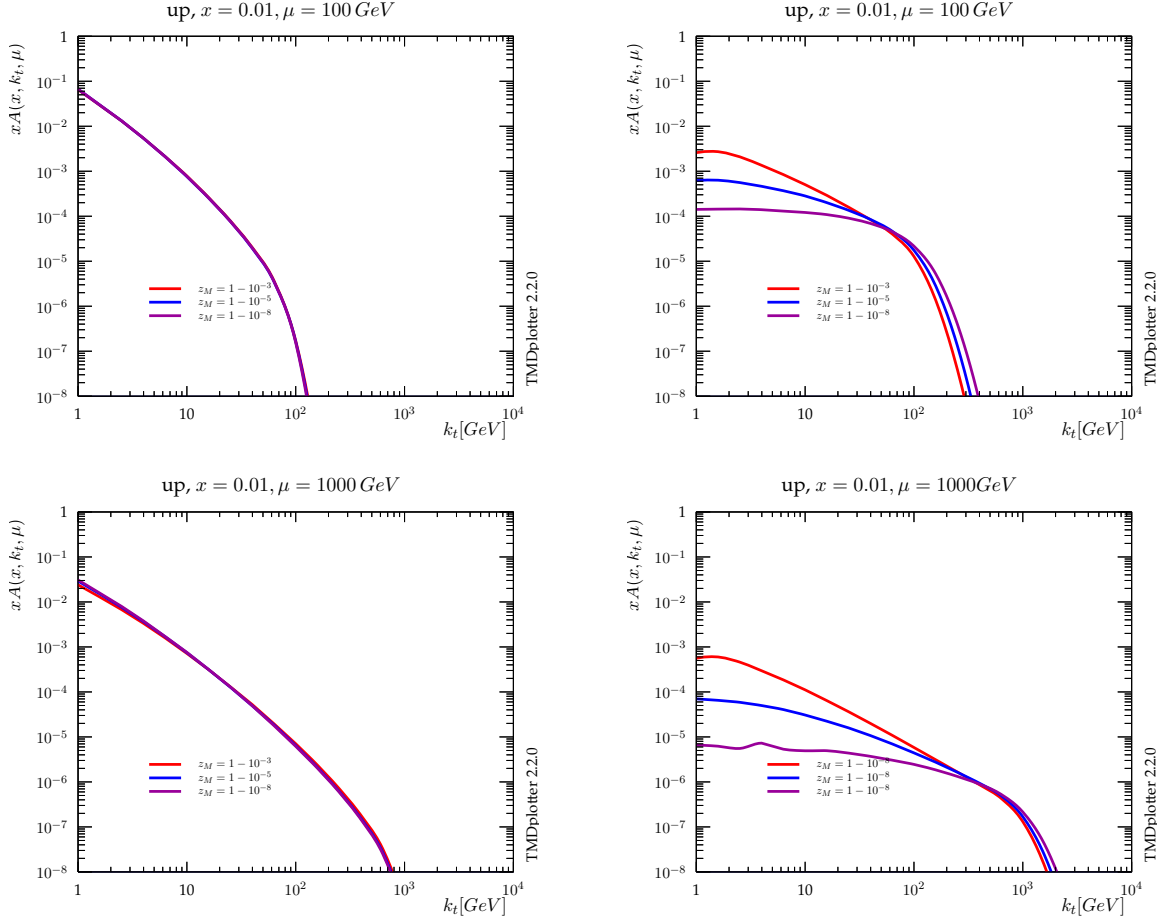


Figure 3: Transverse momentum up-quark distribution at  $x = 10^{-2}$  and  $\mu = 100$  GeV (upper row),  $\mu = 1000$  GeV (lower row) for different values of the resolution scale parameter  $1 - z_M = 10^{-3}, 10^{-5}, 10^{-8}$ : (left) angular ordering; (right) transverse momentum ordering.

In Figs. 2,3 we apply our numerical solution of Eq. (7) to study the transverse-momentum dependence of the gluon and up-quark distribution and their behavior with the soft-gluon resolution parameter  $z_M$ . The parameter  $z_M$  in general depends on the evolution scale  $\mu$ . For numerical illustrations in this paper we limit ourselves to presenting results at fixed values of  $z_M$ . Fig. 2 shows the gluon distribution versus  $k_t \equiv |\mathbf{k}|$  for different values of the resolution parameter,  $1 - z_M = 10^{-3}, 10^{-5}, 10^{-8}$ . Fig. 3 shows analogous curves for the up-quark distribution. The distributions are plotted for a fixed value of longitudinal momentum fraction,  $x = 10^{-2}$ , and two values of evolution scale,  $\mu = 100$  GeV (top panels) and  $\mu = 1000$  GeV (bottom panels).<sup>2</sup> On the right are the results for transverse-momentum ordering; on the left are the results for angular ordering. We see that the transverse-momentum ordering does not lead to results

<sup>2</sup>The plots in Figs. 2,3 are produced using the plotting tool TMDplotter [24, 25].

independent of  $z_M$ . In contrast, the angular ordering does. The different behavior is associated with the emission of gluons at large negative rapidities,  $y \sim \ln(p^+/p^-) \rightarrow -\infty$ . In the case of transverse-momentum ordering, for quantities which are not inclusive but depend on observed transverse momenta, an extra dependence is left over on  $z_M$ , corresponding to a cut-off on the rapidity of emitted gluons. On the other hand, the angular ordering correctly takes into account the cancellation of non-resolvable emissions due to soft-gluon coherence [5], and no dependence is left on the resolution scale.

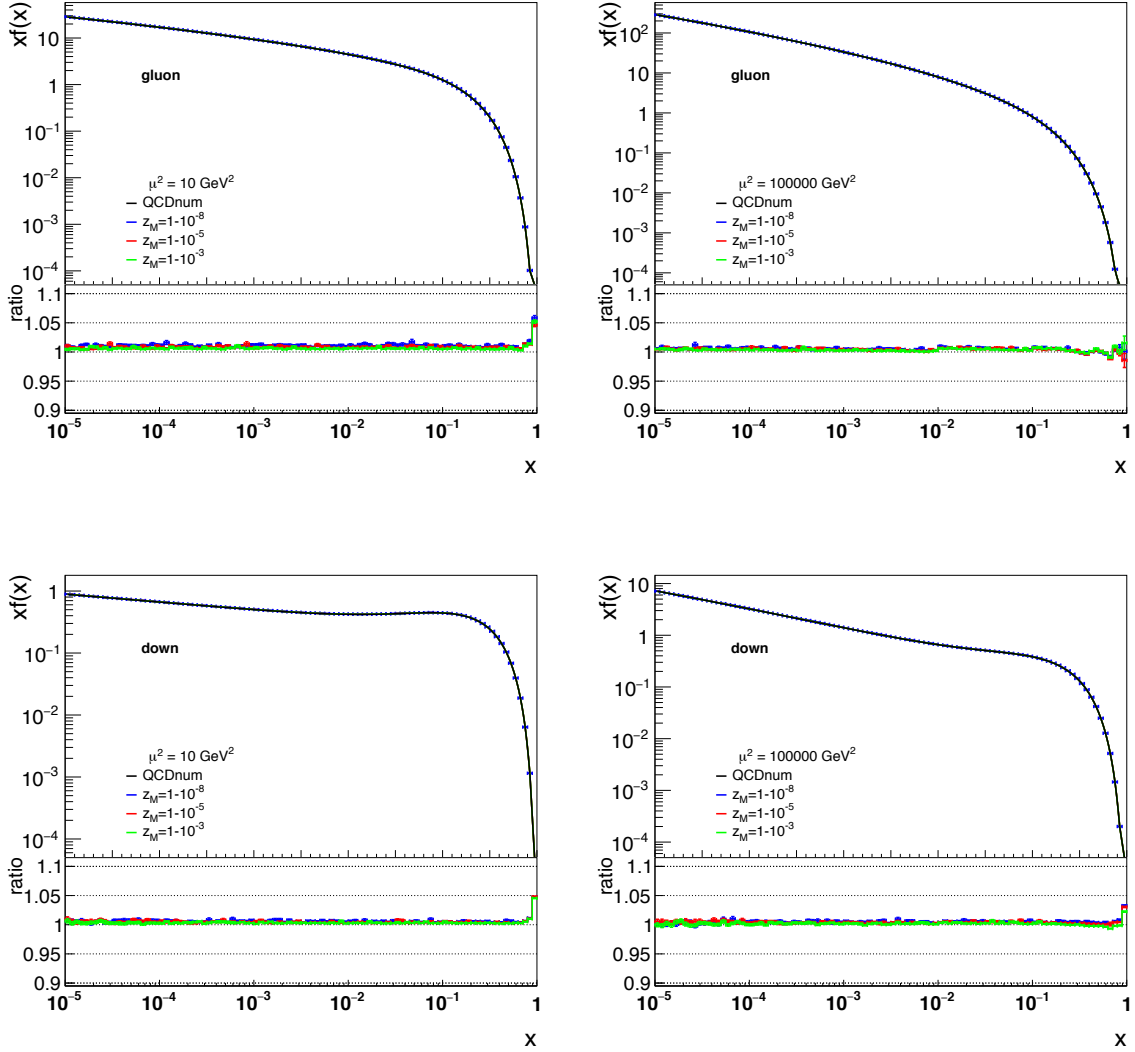


Figure 4: Integrated gluon and down-quark distributions at  $\mu^2 = 10 \text{ GeV}^2$  (left column) and  $\mu^2 = 10^5 \text{ GeV}^2$  (right column) obtained from the parton-branching solution for different values of  $z_M$ , compared with the result from QCDNUM. The ratio plots show the ratio of the results obtained with the parton-branching method to the result from QCDNUM.

We find that the effect from the ordering variable and soft-gluon resolution illustrated in Figs. 2,3 influences the transverse momentum distribution for any kinematic region, namely, both at small  $k_t$  and large  $k_t$ , and for any value of  $x$  (including the low- $x$  region).

The result in Figs. 2,3 is obtained using an arbitrarily chosen form for the distributions at the initial scale of

evolution  $\mu_0$  in Eq. (12). This is sufficient to illustrate the main point about the  $z_M$  dependence. In a complete treatment, the initial distributions are to be determined from fits to experimental data. We plan to report on this in a future publication.

Also, we have obtained the numerical curves in Figs. 2,3 by restricting ourselves to leading order in the strong coupling. The method described in this paper however is general and can be extended to higher orders. Explicit results at the next-to-leading order will be presented in a separate paper.

Fig. 4 shows the result of applying our parton-branching solution of Eq. (7) to compute the evolution of gluon and quark distributions as functions of  $x$ , for different values of the resolution scale parameter  $z_M$ . We use this to validate our method in the case of ordinary parton distributions, integrated over  $k_t$ . As a consistency check we verify that, regardless of the ordering variable in Fig. 2, the result for the inclusive parton distributions converges as a function of  $z_M$  for large enough  $z_M$ . Further, we compare the answer from our parton-branching solution of the evolution equations to semi-analytic results obtained via the evolution package QCDNUM [26–28].<sup>3</sup> We find agreement to a level better than 1 %.

In conclusion, we have shown that the evolution of parton distribution functions can be calculated, including the transverse momentum dependence, from a parton branching approach, provided infrared contributions are treated by a method which takes into account consistently soft gluon emissions near the endpoint  $z \rightarrow 1$  not just at inclusive level but at exclusive level. We have analyzed in detail the dependence on the soft-gluon resolution scale parameter  $z_M$ .

Having defined this properly opens the way to collider applications of TMD parton distributions. Contrary to most studies so far, which are limited to specific kinematic regions, the approach of this paper is expected to be valid more generally and in particular includes the full flavor structure.

**Acknowledgments.** We are grateful to S. Jadach for many fruitful discussions on the topics of this paper. FH acknowledges the support and hospitality of DESY, the University of Hamburg and the DFG Collaborative Research Centre SFB 676 “Particles, Strings and the Early Universe”.

## References

- [1] B. R. Webber, *Ann. Rev. Nucl. Part. Sci.* **36** (1986) 253.
- [2] A. Bassetto, M. Ciafaloni and G. Marchesini, *Phys. Rept.* **100** (1983) 201.
- [3] Y. L. Dokshitzer, V. A. Khoze, S. I. Troian and A. H. Mueller, *Rev. Mod. Phys.* **60** (1988) 373.
- [4] G. Marchesini and B. R. Webber, *Nucl. Phys. B* **310** (1988) 461.
- [5] S. Catani, G. Marchesini and B. R. Webber, *Nucl. Phys. B* **349** (1991) 635.
- [6] R. Angeles-Martinez *et al.*, *Acta Phys. Polon. B* **46** (2015) 2501.
- [7] T. Sjöstrand, arXiv:1608.06425 [hep-ph]; S. Höche, preprint SLAC-PUB-14498 (2011); arXiv:1411.4085 [hep-ph].
- [8] Z. Nagy and D. E. Soper, *JHEP* **1406** (2014) 179.
- [9] S. Dooling *et al.*, *Phys. Rev. D* **87** (2013) 094009; arXiv:1304.7180 [hep-ph]; *Eur. Phys. J. C* **72** (2012) 2254.
- [10] F. Hautmann, *Phys. Lett.* **B655** (2007) 26.
- [11] F. Hautmann *et al.*, in preparation.
- [12] V.N. Gribov and L.N. Lipatov, *Sov. J. Nucl. Phys.* **15** (1972) 438.
- [13] G. Altarelli and G. Parisi, *Nucl. Phys.* **B126** (1977) 298.
- [14] Yu.L. Dokshitzer, *Sov. J. Nucl. Phys.* **46** (1977) 641.
- [15] G. Curci, W. Furmanski and R. Petronzio, *Nucl. Phys.* **B175** (1980) 27.
- [16] W. Furmanski and R. Petronzio, *Z. Phys.* **C11** (1982) 293.
- [17] M. Bengtsson, T. Sjöstrand and M. van Zijl, *Z. Phys.* **C32** (1986) 67.
- [18] T. Sjöstrand and P.Z. Skands, *Eur. Phys. J. C* **39** (2005) 129.
- [19] S. Gieseke, P. Stephens, and B.R. Webber, *JHEP* **0312** (2003) 045.
- [20] F. Hautmann, H. Jung and S. Taheri Monfared, *Eur. Phys. J. C* **74** (2014) 3082.
- [21] F. Hautmann and H. Jung, *Nucl. Phys.* **B883** (2014) 1; arXiv:1206.1796 [hep-ph]; *Phys. Lett.* **B736** (2014) 293.
- [22] F. Hautmann, H. Jung and A. Lelek, *PoS DIS2016* (2016) 036.
- [23] F. Hautmann, *Int. J. Mod. Phys. A* **16S1A** (2001) 238 [hep-ph/0011381].
- [24] F. Hautmann, H. Jung, M. Krämer, P.J. Mulders, E.R. Nocera, T.C. Rogers and A. Signori, *Eur. Phys. J. C* **74** (2014) 3220.
- [25] P. Connor, F. Hautmann and H. Jung, *PoS DIS2016* (2016) 039.
- [26] M. Botje, *Comput. Phys. Commun.* **182** (2011) 490.
- [27] M. Botje, *Eur. Phys. J. C* **14** (2000) 285.

---

<sup>3</sup>Similar comparisons were made in [29, 30] and in [31].

- [28] M. Virchaux and A. Milsztajn, Phys. Lett. B **274** (1992) 221.
- [29] S. Jadach and M. Skrzypek, Acta Phys. Polon. B **35** (2004) 745.
- [30] K. J. Golec-Biernat, S. Jadach, W. Placzek and M. Skrzypek, Acta Phys. Polon. B **37** (2006) 1785.
- [31] H. Tanaka, Prog. Theor. Phys. **110** (2003) 963.